IMPLEMENTATIONS FOR MEMS IN THE VESTIBULAR SYSTEM

V. Manoev, Ts. Kachamachkov

Technical University of Sofia, Bulgaria
Faculty of Telecommunication, TU-Sofia, "Kl. Ohridsky" str. 8, 1000 Sofia, Bulgaria
E-mail: vmanoev@outlook.com

Abstract

This paper presents a feasibility study on an MEMS based implantable vestibular prosthesis. Our end-goal is to design a prosthesis that will replace the function of the damaged vestibular end-organ by providing an MEMS chip that will accurately sense, extract, and transmit 3-dimensional motion information for people who have permanently lost peripheral vestibular function. The prosthesis prototype includes orthogonal triad of accelerometers and gyroscopes on-a-single finger a sized chip. Based on physiological data on perceptual thresholds of linear acceleration and angular velocity in humans, we conclude that the MEMS technology is a viable candidate for such an implant. Functional architecture for the vestibular prosthesis is introduced.

- *Implementations for mems in the vestibular system.*
- *The author has made a thorough research of existing implementations.*
- *Achieving a thorough overview of current implementations for mems in the vestibular system.*

1. INTRODUCTION

The primary function of the vestibular system is to provide the brain with information about the body's motion and orientation. The absence of this information causes blurred vision (oscillopsia), balance difficulties, and spatial disorientation, vertigo, dizzyness, imbalance, nausea, vomiting, and other symptoms often characterize dysfunction of the vestibular system. The symptoms may be quite mild, lasting minutes, or quite severe, resulting in total disability [1]. Sensory prostheses to articially replace lost sensory function for a number of sensory systems are currently under investigation. For example, cochlear implants use electrical stimulation to restore hearing, providing some relief for patients su_ering profound sensori neural hearing loss [2]. Using similar principles, a vestibular prosthesis could provide head orientation information to the nervous system for patients sufiering from peripheral vestibular disorders. At least two categories of vestibular prosthesis might be considered. One approach is to provide the head movement information to the nervous system directly by electrically stimulating the vestibular neural pathways related to spatial orientation. An other approach is to provide the information via sensory substitution through other sensory systems (e.g., tactile, visual, auditory, etc.) [3]. This work falls in the _rst category. Our goal is to develop an implantable, vestibular neural prosthesis using electrical stimulation. To the best of our knowledge, there is only one group working on neural semicircular canal prosthesis [4, 5]. This group has already reported successful interface of the device with vestibular neurons. The group uses an o_-the-shelf single axis piezoelectric vibrating gyroscope to measure the head rotation and to provide corresponding stimulus to the nervous system. The group reported experimental results on an animal model of guinea pigs, in which the gyroscope was mounted externally to the animal's skull using small bolts and miniature stainless-steel screws. Microcontroller was used to convert rotational information in to electrical pulsatile stimulus. [6]

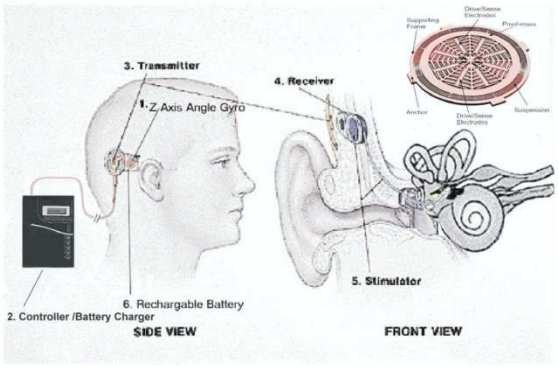

Figure 1. A conceptual model of a totally implantable vestibular prosthesis. The implant is based on 3-axes micro-size gyroscopes integrated alongside with signal conditioning electronic son the same silicon chip

The device includes three main functional units – a sensing unit, a pulse generator, and a stimulator. The device also includes two supporting units: a power supply and an external controller and chargin unit. The sensing unit includes 3-axis accelerometers and 3-axis gyroscopes. These devic-

es sense linear and angular motion of the head and generate voltages proportional to the corresponding linear acceleration and angular velocity. Then, voltages are sent to the pulse generating unit where angular velocities (or linear accelerations) are translated into voltage pulses. In the stimulator, the voltage pulses are converted into current pulses and are delivered through specially designed electrodes to stimulate the corresponding vestibular nerve elements. Each functional block of the chip consumes electrical power. For long term autonomous operation of the implantable device, it is required to supply power externally. Additionally, the implant should be able to communicate with an external controller and charging unit.

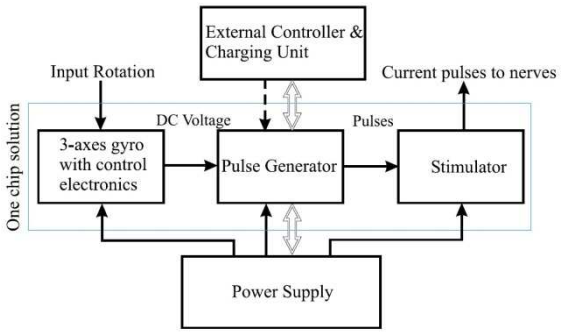

Figure 2. Functional diagram of the vestibular implant [7]

2. EXPERIMENTAL SETUP

The MEMS accelerometer consists of a proof mass suspended by compliant beams anchored to a_xed frame. External acceleration due to motion of the object to which the sensor's frame is attached, displaces the support frame relative to the proof mass, which in turn, changes the initial stress in the suspension spring. Both this relative displacement and the suspension-beam stress can be used as a measure of the external acceleration.

In the most general case, the proof-mass motion can have six degrees of freedom. But typically in a unidirectional accelerometer, the geometrical design of the suspension is such that one of these axes has low sti_-ness while high sti_ness along other axes. For example, in case of the Z-axis accelerometer, the proof mass of the device will displace in out-of-plane of the chip only if there is an acceleration component along the z-axis. Our micromachined gyroscopes use vibrating element to measure rotational velocity based on the Coriolis principle [8]. Just like a linear accelerometer, the micromachined vibrating angular rate sensor consists of a mass suspended on elastic supporting exures anchored to the substrate, Figure 3.

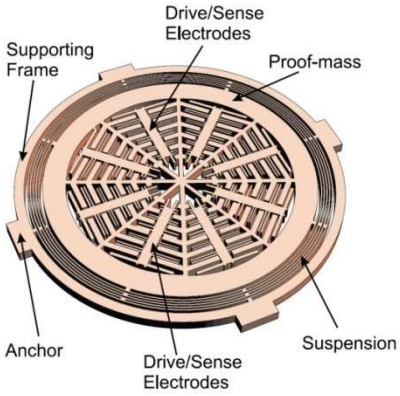

Figure 3. Schematic illustration of a MEMS implementation of the z-axis rate integrating gyroscope. [8]

$$P\left(\frac{d\vec{v}}{dt}+\vec{v}.\nabla\vec{v}\right)=-\nabla p+\mu\nabla^2\vec{v}+\vec{f}\ (1)$$

[9] Where the terms on the left-hand side comprise inertial terms and where the terms on the right-hand side are depending on pressure, viscosity and body forces represented by$\vec{f}$. Since the fluid flow is inside a cylindrical channel, we will use cylindrical coordinates to describe the fluid dynamics. We assume that there are no pressure gradients in the circular channel $(\nabla \mathrm{p}=0)$ and the flow-velocity is only non-zero lthe axial direction z withcomponent v and the tube radius ismuch smaller than the radius of the vestibular circular systemR_c. A harmonic angular acceleration will lead to a body force density$f$ in the axial direction:

$$f_z = PR_c\alpha_{ext}e^{i\omega t} \qquad (2)$$

where $\alpha_{ext}$is the amplitude of a harmonic angular acceleration with frequency ω.The Navier-Stokes equations in (1) can be simplified to

$$\mu\left[\frac{d^2v}{dr^2}+\frac{1}{r}\frac{dv}{dr}\right]+f_z=0 \qquad (3)$$

for Reynold's numbers in the fully laminar flow regime [10]:

$$R_e=\frac{PV_0d}{\mu}<200 \qquad (4)$$

To find a solution for the fluid velocity-profile $v(r,t)$, we assume a harmonic flow with a parabolic profile [11,12]:

$$v(r,t) = V_0 e^{i\omega t}\left(1 - \frac{4r^2}{d^2}\right) \quad (5)$$

Substituting this expression into (3) gives

$$V_0 = \frac{P}{\mu}\frac{R_c d^2}{16}\alpha_{ext} \quad (6)$$

As a result, the flow velocity amplitudeV_0 defined in (6) is valid when

$$\alpha_{ext} < \frac{3200\mu^2}{P^2 d^3 R_c} \quad (7)$$

Following (6), to achieve a sensitive angular acceleration sensor, we need a fluid with a high density P and low viscosity μ to obtain a relatively large fluid flow velocity. Furthermore, the channel should have a large diameter d and the sensor benefits from a large system radius R_c. To demonstrate the sensing capability of our angularacceleration sensor, the setup shown in figure 4 was used and experiments were performed for rotational frequencies within a range of 7–14 Hz. The applied voltageU_s was generated sinusoidally using a Stanford SR 830 lock-in amplifier with its frequency set to 50kHz and the amplitude to 0.7V. The output of the bridge was measured differentially using the lock-in amplifier. Its output was demodulated by setting the amplifier time constant to 3ms and the roll-off to 12dB. The resulting envelope was then band-pass filtered using a Stanford SR 650 filter system with its band-pass set to 1–20Hz, in order to improve the signal-to-noise ratio, and amplified with a gain of 20dB. The filtered output was monitored using an oscilloscope (Agilent DSO1024A) and its RMS-value was measured using a multimeter (Keithley 2001). Using the geometrical properties of the rotational setup, the acceleration amplitude was calculated for every frequency. The obtained results for the measured RMS-voltage are shown in figure 8, together with a linear regression fit. As we observe, the sensor's response is in good agreement with the expected linear response. The calculated full scale error is found to be about 3.9%, with the full-scale set at approximately $2\ x\ 10^5\ ^o s^{-2}$. To verify the sensor's response to angular accelerations, we changed the medium inside the tube from water to air. As a result, the output voltage dropped significantly and no clear sinusoidal waveform was observed when performing measurements identical to those shown in figure 5.

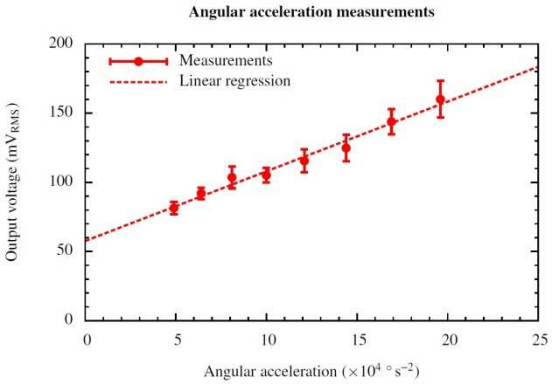

Figure 4: Measured response versus angular accelerationamplitudes. [13,14,15]

ACKNOWLEDGMENTS

The research described in this paper is supported by the Scientific Research Sector of TU-Sofia under the contract No 152пд0054-07

References

[1] R. W. Baloh and G.M. Halmagyi. Disorders of the Vestibular System. Oxford University Press, Oxford, U.K., 1996.

[2] S. U. Ay, F.-G. Zeng, and B. J. Shen. Hearing with Bionic Ears. IEEE Circuits and devices, 5:18{23,1997.

[3] M. Weinberg, J. Borenstein, J. Connelly, A. Kourepenis, P. Ward, and J. Heiertz. Application of draper/ boeing micromechanical inertial instruments. Sensors Expo'98, CSDL-P-3673, 1998. Oct., Chicago, IL.

[4] W. Gong and D. M. Mereld. Prototype Neural Semicircular Canal Prosthesis Using Patterned Electrical Stimulation. Annals of Biomedical Engineering, 28:572{581, 2000.

[5] W. Gong and D. M. Mereld. System Design and Performance of a Unilateral Horizontal Semicircular Canal Prosthesis. IEEE Transactions on Miomedical Engineering, 49(2):175{181, 2002.Feb.

[6] A. Shkel. Micromachined gyroscopes: Challenges, design solutions, and opportunities. 2001 SPIE Annual International Symposium on Smart Structures and Materials, 2001. (Invited Paper)March, 2001, Newport Beach, CA.

[7] I. S. Curthoys. The Response of Primary Horizontal Semicircular Canal Neurons In the Rat And Guinea Pig To Angular Acceleration. Exp. Brain Res, 47:286{294, 1982.

[8] A. Shkel, R. Horowitz, A. Seshia, S. Park and R. T. Howe. Dynamics and control of micromachined gyroscopes. The American Control Conference, June 1999. San Diego, CA.

[9] B. R. Munson, D. F. Young, and T. H. Okiishi, Fundamentals of fluid mechanics, 5th ed., J. Welter, T.

Kulesa, and S. Dumas, Eds. USA: John Wiley & Sons, Inc., 2006.

[10] X. F. Peng, G. P. Peterson, and B. X. Wang, "Frictional flow characteristics of water flowing through rectangular microchannels, "Exp. Heat Transf., vol. 7, no. 4, pp. 249–264, Apr. 1994.

[11] E. R. Damiano and R. D. Rabbitt, "A singular perturbation model of fluid dynamics in the vestibular semicircular canal and ampulla," J. Fluid Mech., vol. 307, pp. 333–372, 1996.

[12] R. Vega, V. V. Alexandrov, T. B. Alexandrova, and E. Soto, "Mathematical model of the cupula-endolymph system with morphological parameters for the axolotl (ambystoma tigrinum) semicircular canals," Open Med. Inform. J., vol. 2,pp. 138–148, 2008.

[13] T. S. J. Lammerink, N. R. Tas, M. Elwenspoek, and J. H. J. Fluitman, "Micro-liquid flow sensor," Sens. Act. A, vol. 37–37, pp. 45–50, 1993.

[14] ST Microelectronics, "LIS1R02 (L6671)," 2002, Angular accelerometer.

[15] Endevco, "Model 7302BM4 – Piezoresistive angular accelerometer," 2009.

[16] J. J. Groen and L. B. W. Jongkees, "The threshold of angular acceleration perception," J. Physiol., vol. 107, pp. 1–7, 1948.